Long-distance propagation of pseudo-partially coherent Gaussian Schell-model beams in atmospheric turbulence*

Qian Xian-Mei(钱仙妹)†, Zhu Wen-Yue(朱文越), and Rao Rui-Zhong(饶瑞中)

Key Laboratory of Atmospheric Composition and Optical Radiation of Chinese Academy of Sciences, Anhui Institute of Optics and Fine Mechanics, Chinese Academy of Sciences, Hefei 230031, *China*

(Received 23 November 2011; revised manuscript received 12 February 2012)

Propagation properties of spatially pseudo-partially coherent Gaussian Schell-model beams through the atmospheric turbulence over a long-distance uplink path are studied by numerical simulation. A linear coordination transformation is introduced to overcome the window effect and the loss-of-resolution problem. The beam spreading, beam wandering, and intensity scintillation as functions of turbulence strength, source correlation length, and change frequency of random phase that models the partial coherence of the source are analyzed. It is found that the beam spreading and the intensity scintillation of the partially coherent beam are less affected by the turbulence than those of the coherent one, but it suffers from severer diffractive effect, and the change frequency of random phase has no evident influence on it. The beam wandering is insensitive to the variation of source correlation length, and decreases firstly then goes to a fixed value as the change frequency increases.

Keywords: long-distance propagation, pseudo-partially coherent Gaussian Schell-model beam, atmospheric turbulence, numerical simulation

PACS: 42.25.Bs, 42.25.Kb, 92.60.Ta, 92.60.hk **DOI:** 10.1088/1674-1056/21/9/094202

1. Introduction

It is widely accepted that distortions due to random variation in the refractive index of atmospheric turbulence, such as beam wandering, beam spreading, and scintillation, have significant adverse effects on many applications of laser engineering, such as remote sensing, tracking, and optical communications.[1−4] The turbulence-induced intensity fluctuation and the beam wandering at the receiver result in the rise of system bit error rate and tracking error, respectively, and the beam spreading may decrease the power and the power density at the receiver, which are unsatisfactory in most applications. And the fully coherent laser beams are very sensitive to the distortions of atmospheric turbulence. Consequently, these adverse effects become main restricted factors of the improvement of system performance. Hence, there has been growing interest in developing techniques to overcome the turbulent effects, and it would be useful to utilize new beams that are affected as little as possible by the presence of atmospheric turbulence. Recently, there were many theoretical researches on the propagation effects of partially coherent beams (PCBs) in turbulence, and the results indicated that PCBs are less affected by the turbulence than the fully coherent beams (CBs).[5−13] Some experiments also suggested that the use of a partially coherent beam source does reduce the intensity scintillation at the receiver.[14−16]

The partially coherent Gaussian Schell-model (GSM) beam is a typical spatially partially coherent beam, which has been intensively studied in some publications. But it is very difficult and not necessary to generate a fully-developed GSM beam. A more practical beam, the pseudo-partially coherent beam (PPCB), was proposed.[17] A PPCB can be generated by sending a CB through a random phase screen that changes a few times during the time within which the atmospheric turbulence has changed once. The propagation effects of beam spreading, beam wandering, and intensity fluctuation on PPCBs through the turbulence were studied in Refs. [17]–[19]. However, most previous works were concentrated on the short-distance propagation. The case of long-distance propagation, which is involved in many applications, such

*Project supported by the National Natural Science Foundation of China (Grant Nos. 61107066 and 40805006).

†Corresponding author. E-mail: qianxianmei@aiofm.ac.cn

© 2012 Chinese Physical Society and IOP Publishing Ltd

as satellite–ground laser communications, was seldom studied. On the other hand, the change frequency of the random phase, which models the partial coherence of the source, is an important parameter in generating a PPCB, but little attention has been paid to the effects induced by the variation of the change frequency.

In this paper, propagation properties of spatially pseudo-partially coherent Gaussian Schell-model beams through the turbulent atmosphere along a long-distance uplink path up to hundreds of kilometers are investigated by using wave optics numerical simulation. A linear coordinate transformation applied to the simulation of long-distance propagation is presented to overcome the window effect and the loss-of-resolution problem. In Section 2, the basic parameters and properties of spatially pseudo-partially coherent Gaussian Schell-model beams are introduced. In Section 3, the approach for the numerical simulation of the propagation process of PPCBs is presented, and the linear coordinate transformation is introduced. Then the influences of turbulence strength, source correlation length, and change frequency of random phase on the beam spreading and the beam wandering are analyzed statistically in Section 4. The intensity scintillation property of the PPCB is studied in Section 5. Finally, in Section 6, we give some discussion and summarize the main results.

2. Basic parameters

As proposed in many publications, the partial coherence can be modeled by a diffuser or a random phase assumed to be $\phi(x,y;t)$, and the initial optical field of a partially coherent beam can be expressed as

$$E(x,y,z=0;t) = E_0(x,y,z=0) \times \exp[\mathrm{i}\phi(x,y;t)], \quad (1)$$

where $E_0(x,y,z=0)$ is the initial optical field of the corresponding fully coherent beam. For a spatially partially coherent GSM beam, the random phase satisfies the Gaussian spatial coherence function, and can be described by a random signal convoluted with a Gaussian distributed function[20]

$$\phi(x,y;t) = r(x,y;t) \otimes g(x,y), \quad (2)$$

where $r(x,y;t)$ is the spatially uncorrelated random signal with a standard deviation σ_r, and $g(x,y)$ is a Gaussian function with standard deviation σ_g

$$g(x,y) = \frac{1}{2\pi\sigma_\mathrm{g}^2}\exp\Big(-\frac{x^2+y^2}{2\sigma_\mathrm{g}^2}\Big). \quad (3)$$

The lateral correlation length l_c is introduced to describe the spectral degree of coherence, which is given by

$$l_\mathrm{c}^2 = \frac{16\pi\sigma_\mathrm{g}^4}{\sigma_\mathrm{r}^2}. \quad (4)$$

For a fully coherent beam, l_c goes to infinite, and the degree of source coherence degrades as l_c decreases.

The random phase $\phi(x,y;t)$ is representative of the phase modulation of a coherent beam source. The changing frequency of $\phi(x,y;t)$ is often described by the relative modulation frequency K compared with the change of atmospheric turbulence. It means that during the period that the atmospheric turbulence has changed once, the random phase has changed K times. The main difference between the partially coherent and the pseudo-partially coherent GSM beams is the change frequency of $\phi(x,y;t)$. For the partially coherent beams, the change frequency is infinite, but for the pseudo-partially coherent beams, the change frequency is often chosen to be several times of the frequency of the turbulent fluctuation. So we point out that the propagation properties of the pseudo-partially coherent GSM beams may not follow the fully-developed partially coherent GSM theory under all conditions.

3. Numerical simulation method

Based on the Maxwell equation and the parabolic approximation, the optical field in turbulent media satisfies the following equation:

$$2\mathrm{i}k\frac{\partial E}{\partial z} + \boldsymbol{\nabla}_\perp^2 E + 2k^2 n_1 E = 0, \quad (5)$$

where $k = 2\pi/\lambda$ is the wave number, and n_1 is the variation of the refractive index. The multiple-phase screen method[21] is used to solve Eq. (5) and to simulate the propagation processes of beam in free space and in the turbulent atmosphere. Considering the concept of pseudo-partially coherent GSM beam, we use the approach described in Refs. [19] and [20] to generate GSM beams and to get each realization of the intensity field at the receiver, based on which the beam spreading and the beam wandering are analyzed statistically.

For the long-distance propagation, the beam size at the receiver may be tens or hundreds of times larger than that at the transmitter due to the strong diffractive effect. If the numerical mesh keeps the same at each turbulent phase screen, the light beam at the transmitter could not be sampled sufficiently, or the

light beam at the receiver would collide with the edge of the phase screen, i.e., the window effect, both would result in a low simulation precision. So the grid interval should be varied according to the beam size at different turbulent phase screen to overcome the window effect and the loss-of-resolution problem. We use the coordinate transformation to achieve this purpose. The schematic diagram of coordinate transformation is shown in Fig. 1. At the first phase screen of transmitter, the size of phase screen is assumed to be $L_0 \times L_0$, and that of the last phase screen at the receiver is assumed to be $L_1 \times L_1$, L_0 and L_1 should be at least several times of the sizes of the light beams at the transmitter and the receiver, respectively. The linear coordinate transformation is used, and the coordinate transformation factor $D(z)$ at position z can be given by

$$D(z) = \frac{L_z}{L_0} = 1 + \frac{z}{L}\Big(\frac{L_1}{L_0} - 1\Big) = 1 - \delta z, \quad (6)$$

where L is the propagation length, and

$$\delta = -\frac{1}{L}\Big(\frac{L_1}{L_0} - 1\Big).$$

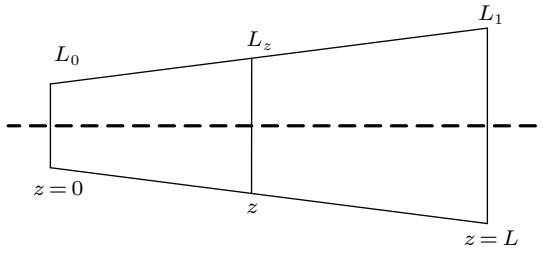


Fig. 1. Schematic diagram of coordinate transformation.

Consider a new Cartesian coordinate system (x', y', z') defined by

$$x' = x/D(z), \quad y' = y/D(z), \quad z' = \frac{1}{\delta}\Big(\frac{1}{1-\delta z} - 1\Big),$$

and assume the relation between optical field $E_{\rm T}(x', y', z')$ in the new coordinate system and that in the original coordinate system satisfies

$$E(x, y, z) = \frac{1}{D(z)} E_{\rm T}(x', y', z') \exp[{\rm i}\xi(x, y, z)], \quad (7)$$

where

$$\xi(x, y, z) = -\frac{k[1 - D(z)]}{2zD(z)}(x^2 + y^2),$$

then the parabolic equation can be written as

$$2{\rm i}k\frac{\partial E_{\rm T}}{\partial z'} + \nabla_{\perp}'^2 E_{\rm T} + 2k^2 n_1 D^2 E_{\rm T} = 0. \quad (8)$$

Equation (8) is similar to Eq. (5). Thus we can use the same simulation algorithm to solve Eq. (8), and the variation of refractive index becomes $n_1 D^2$ in the new coordinate system. Set the numerical grid interval in the new coordinate system to be $\Delta x' = L_0/N$ at all turbulent phase screens, $N \times N$ is the number of grids in the numerical mesh, and $L_0 \times L_0$ is the simulation window dimension. Therefore in the original coordinate system, the grid interval is transformed to be $\Delta x = D(z)\Delta x'$, which changes according to the beam size at different position by factor $D(z)$.

The simulation of light propagation is carried out in the new coordinate system by using the classical split-step Fourier algorithm.[21] Unlike in the original coordinate system, the phase fluctuation spectrum $\Phi_{\Delta S_n'}$ of the thin turbulent phase screen is related to the power spectrum of the fluctuation of refractive index, Φ_n, through the expression

$$\begin{aligned}&\Phi_{\Delta S_n'}(K_{x'}, K_{y'})\\ &= 2\pi k^2 D^4 \Delta z' \Phi_n(K_{x'}, K_{y'}, K_{z'} = 0)\end{aligned} \quad (9)$$

in the new coordinate system based on Eq. (8), where $K_{x'}$, $K_{y'}$, $K_{z'}$ are the wave number coordinates, and $\Delta z'$ is the separation between the phase screens. And the propagation length in the (x', y', z') system is transformed from L to L', which satisfies

$$L' = \frac{1}{\delta}\Big(\frac{1}{1-\delta L} - 1\Big) = \frac{L}{1-\delta L}. \quad (10)$$

After obtaining the optical field $E_{\rm T}(x', y', z' = L')$, the real optical field $E(x, y, z = L)$ in the original coordinate system can be obtained through Eq. (7).

4. Beam spreading and beam wandering

The propagation paths involved in this paper are all vertical uplinks, the Kolmogorov spectrum of turbulence and the HV-5/7 profile of construct constant of refractive index are assumed. The wavelength of the beam is 1.0 μm, and the initial beam radius at the transmitter is 100 mm. Each data point in the following figures and tables is the statistic average result of 100 simulation realizations.

4.1. Turbulence strength

The HV-5/7 profile of construct constant of refractive index used here can be expressed as

$$\begin{aligned}C_{n,\text{HV-5/7}}^2(h) =& 8.2 \times 10^{-26}(21)^2 h^{10}\,{\rm e}^{-h}\\ &+ 2.7 \times 10^{-16}\,{\rm e}^{-\frac{h}{1.5}}\\ &+ 1.7 \times 10^{-14}\,{\rm e}^{-10h},\end{aligned} \quad (11)$$

where h is the altitude from the ground. But in this paper, we assume a C_n^2 profile that is normalized to the construct constant of refractive index at ground $C_{n,0}^2$, which is utilized to define the strength of turbulence. Thus, the assumed C_n^2 profile can be expressed as

$$C_n^2(h) = \frac{C_{n,0}^2}{C_{n,\text{HV-5/7}}^2(h=0)} C_{n,\text{HV-5/7}}^2(h). \qquad (12)$$

Although equation (12) is not suitable for describing the real C_n^2 profile, it is a feasible way to study the influence of turbulence strength on the propagation property.

Set $C_{n,0}^2$ to be 1×10^{-16} m$^{-2/3}$, 5×10^{-16} m$^{-2/3}$, 1×10^{-15} m$^{-2/3}$, 5×10^{-15} m$^{-2/3}$, 1×10^{-14} m$^{-2/3}$, 5×10^{-14} m$^{-2/3}$, and 1×10^{-13} m$^{-2/3}$ respectively, and the propagation length L is chosen to be 100 km. In the new coordinate system (x', y', z'), the grid interval $\Delta x'$ is set to be $\Delta x' = 10W_0/N$, where $N = 256$. For PPCBs, the relative modulation frequency of $\phi(x, y; t)$ is assumed to be $K = 10$, and the source correlation length is $l_c = 1$ cm. Figure 2(a) shows the beam radii of PPCB and CB each as a function of $C_{n,0}^2$, and figure 2(b) shows the relative beam spreading, which is defined by $W_{\text{eff}}/W_{\text{eff0}}$, where W_{eff} and W_{eff0} are the beam radii in the turbulence and in the vacuum, respectively. It can be seen that the beam radius of PPCB is much larger than that of CB, which indicates that the diffractive effect of the PPCB is more serious than that of the CB. However, as the turbulence strength grows, the beam radius of the PPCB increases much more slowly than that of the CB. Even when $C_{n,0}^2 = 1\times10^{-13}$ m$^{-2/3}$ (Rytov index is 36.2), the relative beam spreading of the PPCB is only 1.12, while that of the CB grows to 5.9. This means that the beam spreading of the PPCB is not very sensitive to the distortion of the atmospheric turbulence, and the PPCB is less affected by the turbulence than the CB.

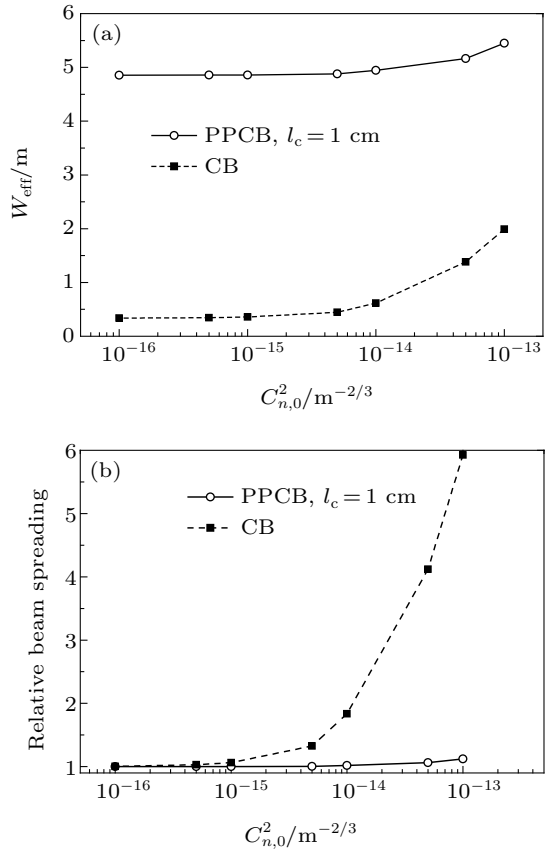


Fig. 2. (a) Beam radii and (b) relative beam spreadings of PPCB and CB versus $C_{n,0}^2$ over a propagation distance of 100 km in turbulence.

Figure 3 shows the beam wanderings of PPCB and CB each as a function of the turbulence strength, where the y axis denotes the root of mean square (RMS) σ_ρ of the wandering of beam centroid. We can see that as the turbulence strength grows, the RMS of beam wandering of the PPCB rises rapidly. When $C_{n,0}^2 = 1\times10^{-13}$ m$^{-2/3}$, σ_ρ rises up to 0.61 m. The beam wandering of the PPCB is almost the same as that of the CB. However, at low $C_{n,0}^2$, the beam wandering of the PPCB is a little larger than that of the CB. As the turbulence strength grows, the difference tends to disappear. For the PPCB, the beam wandering is caused by two kinds of disturbances, the limited randomicity of random phase $\phi(x, y; t)$ and the atmospheric turbulence. So even in vacuum, there is also some extend of beam wandering of the PPCB (it can also be seen in Fig. 6), whereas the beam wandering of the CB is zero in vacuum. This causes the little larger beam wandering of the PPCB at low $C_{n,0}^2$.

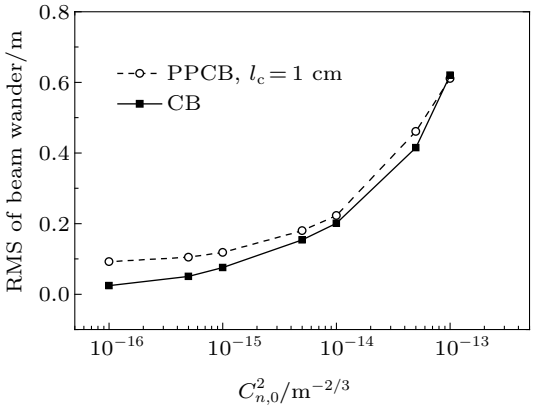


Fig. 3. RMS of beam wanderings of PPCB and CB versus $C_{n,0}^2$ over a propagation distance of 100 km in turbulence.

For the propagation length of 500 km, Table 1 displays the beam radius $W_{\rm eff}$, the relative beam spreading $W_{\rm eff}/W_{\rm eff0}$, the RMS of beam wandering σ_ρ, and the Rytov index σ_1^2 when $C_{n,0}^2$ is chosen to be 1×10^{-16} m$^{-2/3}$, 1×10^{-15} m$^{-2/3}$, 1×10^{-14} m$^{-2/3}$, and 1×10^{-13} m$^{-2/3}$ respectively. It can be seen that the beam radius grows very slowly with the increase of the turbulence strength. Even when the Rytov index goes up to 139.3, the relative variation of the beam radius is less than 23%. But the RMS of beam wandering increases from 0.45 m to 3.15 m when the Rytov index rises from 0.139 to 139.3. Therefore, the beam wandering of the PPCB is affected more severely by the turbulent distortion than the beam spreading.

Table 1. Beam spreading and beam wandering of PPCB versus $C_{n,0}^2$ over a propagation distance of 500 km.

$C_{n,0}^2$/ m$^{-2/3}$	1×10^{-16}	1×10^{-15}	1×10^{-14}	1×10^{-13}
$W_{\rm eff}$/m	24.19	24.23	24.54	27.23
$W_{\rm eff}/W_{\rm eff0}-1$	7.3%	7.5%	8.8%	20.8%
σ_ρ/m	0.45	0.62	1.14	3.15
σ_1^2	0.139	1.39	13.9	139.3

4.2. Source correlation length

Set $C_{n,0}^2=1\times10^{-14}$ m$^{-2/3}$, chose the source correlation length $l_{\rm c}$ of the PPCB to be 0.5 cm, 1 cm, 2 cm, 3 cm, 4 cm, 5 cm, and 6 cm respectively, and assume $K=10$. Figure 4 shows the variations of beam radius in vacuum and in turbulence each as a function of $l_{\rm c}$ over a propagation distance of 100 km. We note that the increase of the source correlation length causes a significant decline of the beam radius, and the beam radius in turbulence is only a little larger than that in vacuum. Under the same condition, the short-term beam radii of the corresponding CB in vacuum and in turbulence are 0.33 m and 0.56 m, respectively. It is clearly revealed that a pseudo-partially coherent Gaussian Schell-model beam has severer diffractive effects than the corresponding coherent Gaussian beam. Though the relative beam spreading of a partially coherent beam is less susceptible to the turbulence (Fig. 2), the turbulent beam radius of a partially coherent beam is generally still larger than that of a coherent beam due to the larger spreading in vacuum.

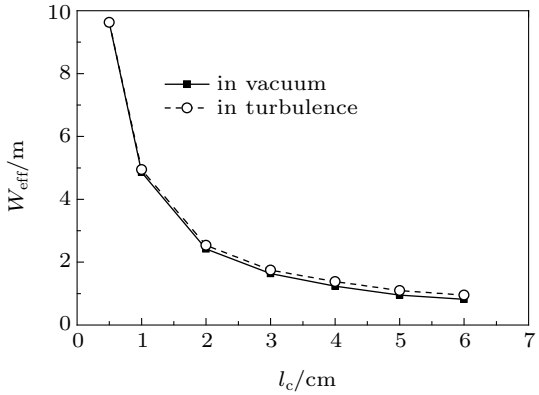


Fig. 4. Beam radii in vacuum and in turbulence of the PPCB versus $l_{\rm c}$ over a propagation distance of 100 km.

In Table 2, the RMS of beam wandering is illustrated with the variation of $l_{\rm c}$, and the last column denotes the RMS of beam wandering of the corresponding CB. It can be seen clearly that the change of $l_{\rm c}$ does not lead to an evident variation of the beam wandering. The average relative variation is less 4%. The beam wandering of the PPCB is almost the same as that of the CB. This indicates that the beam wandering of the PPCB is not sensitive to the degree of source coherence.

Table 2. RMS of beam wandering versus $l_{\rm c}$ over a propagation distance of 100 km.

$l_{\rm c}$/cm	0.5	1.0	2.0	3.0	4.0	5.0	6.0	CB
σ_ρ/m	0.236	0.223	0.224	0.234	0.225	0.249	0.245	0.226

Change the propagation length to be $L=500$ km, and all the other parameters are kept the same as those in Fig. 4. Table 3 shows the beam radii, the relative variations of beam radius, and the beam wanderings with different source correlation lengths. There is a quick decline of beam radius as the source becomes more coherent. But at the same time, the relative variation of beam radius (data in the forth row of Table 3) keeps a noticeable rise. When $l_{\rm c}=0.5$ cm, the relative variation of beam radius is only 6.5%, when $l_{\rm c}=6$ cm, it grows to 23.0%, and it becomes 70.0% for the CB. It means that the beam spreading due to the turbulent distortion is weakened by using partially coherent beams. However, the severe diffractive effect in vacuum causes significant reductions of power and power density at the receiver, which may be an unsatisfactory property in some applications. Thus, the utilization of partially coherent beams and to which extent partially coherent beams are used may depend on the real requirements. From this table, we also see that the beam wandering is almost independent of the source correlation length.

Table 3. Beam radius and wandering versus l_c over a propagation distance of 500 km.

l_c/cm	0.5	1.0	2.0	3.0	4.0	5.0	6.0	CB
W_{eff0}/m	45.02	22.55	11.36	7.67	5.85	4.77	4.07	1.59
W_{eff}/m	47.96	24.54	12.62	8.77	6.88	5.75	5.01	2.70
$W_{eff}/W_{eff0}-1$	6.5%	8.8%	11.1%	14.4%	17.7%	20.5%	23.0%	70%
σ_ρ/m	1.14	1.14	1.15	1.15	1.09	1.11	1.05	1.03

4.3. Modulation frequency

According to the concept of PPCB, besides the turbulence, $\phi(x, y; t)$ may also bring some distortion to the intensity pattern because of its limited randomicity. Thus, the relative modulation frequency K is an important parameter for the generation of the PPCB, and the change of K may cause some variations of beam spreading and beam wandering both in vacuum and in atmospheric turbulence.

Figure 5(a) gives the beam radii in vacuum and in turbulence ($C_{n,0}^2 = 1 \times 10^{-14}$ m$^{-2/3}$) each as a function of K, figure 5(b) shows the relative variation of beam radius compared to the average value. Input parameters are $L = 100$ km and $l_c = 1$ cm. We can see that the beam radius fluctuates around the average value, but the largest relative variation is less than 0.7%. The change of modulation frequency may not cause any obvious variation of beam radius of the PPCB both in vacuum and in atmospheric turbulence.

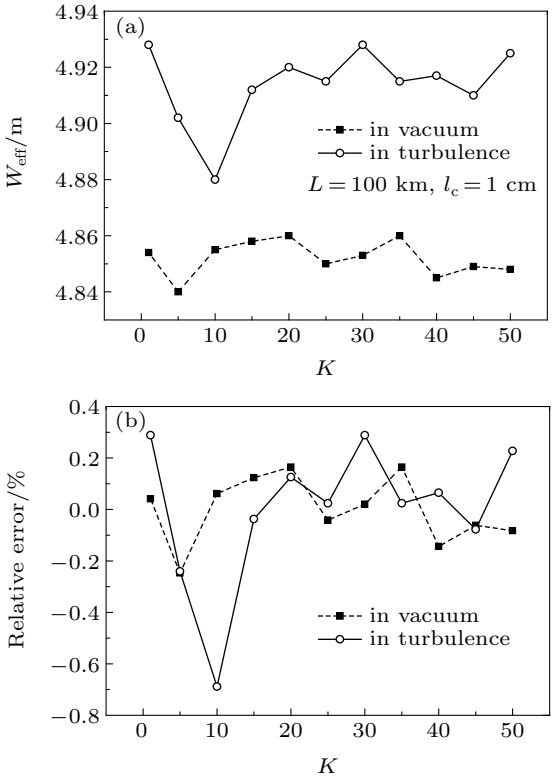


Fig. 5. (a) Beam radii and (b) relative variations of beam radius of PPCBs compared to the average value.

Due to the limited modulation frequency, even in vacuum, there also has some beam wandering. Figure 6 illustrates the RMS of beam wanderings in vacuum and in turbulence each as a function of K. In vacuum, there is a great beam wandering $\sigma_\rho = 0.28$ m when $K = 1$. But with the increase of K, the beam wandering declines quickly, and it is less than 0.05 m when $K = 50$. And it can also be predicted that the beam wandering keeps going down to zero when K approaches infinite, because the fully-developed partially coherent beams have no beam wandering in vacuum. In turbulence, the beam wandering is larger than that in vacuum due to the additional influence of the turbulent distortion. We can see that the effect of partial coherence on the beam wandering is larger than that of the turbulence at $K = 1$. But after K increases to 5, the turbulence is the dominant contribution to the beam wandering, and the beam wandering fluctuates slightly around an average value of 0.226 m. Thus, to some extent, it can be said that beam wandering is insensitive to the modulation frequency of random phase $\phi(x, y; t)$ when $K > 5$ in turbulence.

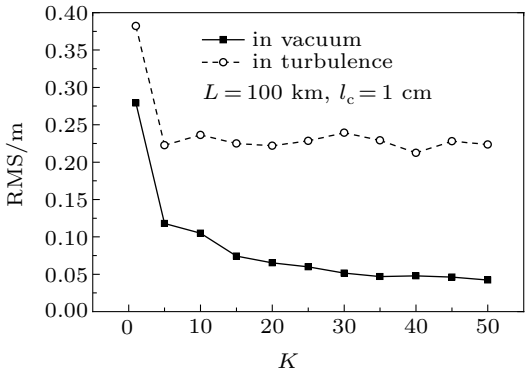


Fig. 6. RMS of beam wanderings in vacuum and in turbulence versus K.

5. Intensity scintillation

The property of intensity scintillation is an important factor for evaluating the performance of free-space light communications. Set the coherence length of the PPCB to be $l_c = 1$ cm, $L = 100$ km, and $C_{n,0}^2 = 5 \times 10^{-16}$ m$^{-2/3}$, 1×10^{-14} m$^{-2/3}$, 5×10^{-14} m$^{-2/3}$, and 1×10^{-13} m$^{-2/3}$ respectively. Figure 7 shows the

off-axis scintillation index as a function of the normalized off-axis distance and the turbulence strength, where ρ is the off-axis distance, and W_{eff0} is the beam radius in vacuum. It can be seen that the scintillation index increases as the turbulence grows stronger. However, even when $C_{n,0}^2 = 1\times10^{-13}$ m$^{-2/3}$, the scintillation index is less than 1, which indicates that the partially coherent beam is insensitive to the turbulent fluctuation.

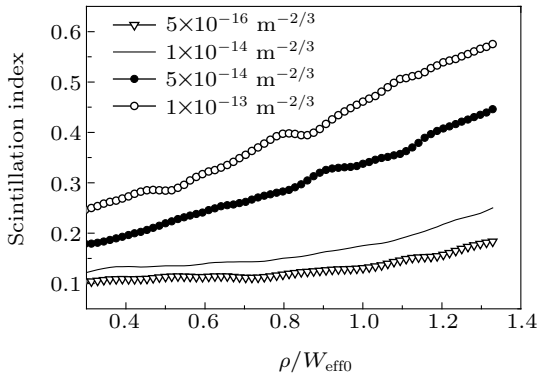


Fig. 7. Off-axis scintillation index versus $C_{n,0}^2$ and normalized off-axis distance.

Figure 8 illustrates the off-axis scintillation index as a function of coherence length l_{c} when $C_{n,0}^2 = 1\times10^{-14}$ m$^{-2/3}$ and L=500 km. We can see that as the coherence length decreases, the scintillation index decreases rapidly. It means that the degradation of beam coherent degree may cause less intensity fluctuation.

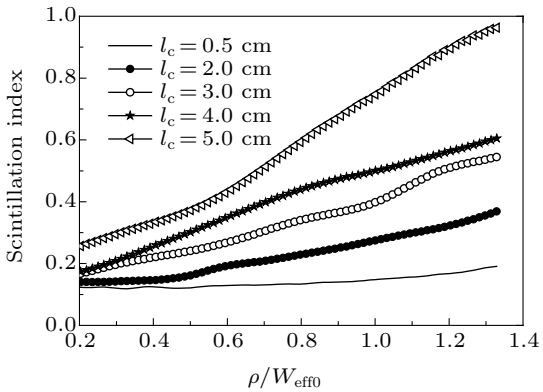


Fig. 8. Off-axis scintillation index versus l_{c} and normalized off-axis distance.

6. Conclusion

Using the wave optics numerical simulation, we have studied the characteristics of spatially pseudo-partially coherent Gaussian Schell-model beams propagating through the atmospheric turbulence over long distances up to 500 km. To overcome the window effect and the loss-of-resolution problem, we have proposed a method of linear coordinate transformation.

The properties of beam spreading, beam wandering, and intensity scintillation of PPCBs as functions of turbulence strength, source correlation length, and change frequency of random phase were examined. It was found that the beam radius of the PPCB increases very slowly as the turbulence strength grows for several orders of magnitude, but increases quickly with the degradation of the source coherence. This means that the beam spreading of the PPCB is not very sensitive to the turbulent distortion but is sensitive to the diffractive effect. Unlike the beam spreading, the beam wandering of the PPCB increases as the turbulence strength grows just like the behavior of the CB, and almost does not change with the variation of the source correlation length. This indicates that the beam wandering of the PPCB is insensitive to the degree of source coherence. The scintillation index of the PPCB decreases evidently as the beam becomes less coherent, and this property can be used to improve the signal-to-noise ratio and reduce the bit error of light communications. As the change frequency varies, there is no evident change of the beam radius either in vacuum or in turbulence. However, even in vacuum, there is also a significant beam wandering when $K = 1$. But as K increases, the beam wandering quickly declines and becomes zero once K goes to infinite. Whereas in turbulence, the beam wandering declines to a fixed value for $K > 5$.

Therefore, form the point of view of beam wandering, the partially coherent beams have no advantage over the coherent ones. The beam spreading and the intensity scintillation of the partially coherent beam are less affected by the turbulence than those of the coherent beam. This may be one of the most important properties of the partially coherent beams that could be utilized to improve the performance of laser engineering. But the partially coherent beams have larger beam radii, which result in lower power density and may be unsatisfactory in some particular applications. So to which extent a partially coherent beam is used and the selection of optimal beam should depend on the real requirements.

References

[1] Khmelevtsov S S 1973 *Appl. Opt.* **12** 2421
[2] Flatte S M and Wang G Y 1993 *J. Opt. Soc. Am.* A **10** 2363

[3] Shelton J D 1995 *J. Opt. Soc. Am.* A **12** 2172
[4] Andrews L C, Phillips R L, Sasiela R J and Parenti R 2005 *Proc. SPIE* **5793** 28
[5] Leader J C 1979 *J. Opt. Soc. Am.* A **69** 73
[6] Gbur G and Wolf E 2002 *J. Opt. Soc. Am.* A **19** 1592
[7] Ricklin J C and Davidson F M 2002 *J. Opt. Soc. Am.* A **19** 1794
[8] Shirai T, Dogariu A and Wolf E 2003 *J. Opt. Soc. Am.* A **20** 1094
[9] Dogariu A and Amarande S 2003 *Opt. Lett.* **28** 10
[10] Korotkova O, Andrews L C and Phillips R L 2004 *Opt. Eng.* **43** 330
[11] Ji X L 2011 *Acta Phys. Sin.* **60** 064207 (in Chinese)
[12] Zhang Y T, Ji X L and Lu B D 2009 *Chin. Phys.* B **18** 571
[13] Cang J and Zhang Y X 2009 *Acta Phys. Sin.* **58** 2444 (in Chinese)
[14] Polejaev V I and Ricklin J C 1998 *Proc. SPIE* **3432** 103
[15] Ricklin J C, Davidson F D and Weyrauch T 2001 *Proc. SPIE* **4538** 13
[16] Dogariu A and Amarande S 2003 *Opt. Lett.* **28** 10
[17] Voelz D and Fitzhenry K 2004 *Proc. SPIE* **5550** 218
[18] Xiao X and Voelz D 2006 *Proc. SPIE* **6304** 63040L-1
[19] Qian X M, Zhu W Y and Rao R Z 2009 *Opt. Express* **17** 3782
[20] Xiao X and Voelz D 2006 *Opt. Express* **14** 6986
[21] Coles W A, Filice J P, Frehlich R G and Yadlowsky M 1995 *Appl. Opt.* **34** 2089